Effects of Nb Surface and Ti Interface Layers on Thermal Stability and Electrical Resistivity of Ag Thin Films

Ziyang Zhang, Midori Kawamura*, Yoshio Abe, and Kyung Ho Kim

Department of Materials Science and Engineering, Kitami Institute of Technology, Kitami, Hokkaido 090-8507, Japan

Nb/Ag, Ag/Ti, and Nb/Ag/Ti films were prepared by rf magnetron sputtering to investigate the effects of the Nb surface and Ti interface layers on the thermal stability and electrical resistivity of 100-nm-thick Ag thin films. The Nb surface layer, regardless of the chemical state of metal or oxide, prevented the migration of Ag atoms during annealing, which contributed to the agglomeration suppression of Ag films. Ti interface layers not only improved the adhesion of Ag films to SiO_2 substrates but also impelled the overcoated Ag atoms to arrange along the close-packed plane (111); thus, Ag/Ti films exhibited relatively good thermal stability and low resistivity. By combining the roles of the Nb surface and Ti interface layers, Nb (5 nm)/Ag (100 nm)/Ti (3 nm) films showed the highest thermal stability and the lowest resistivity. Different materials of surface and interface layers might be more effective for improving the thermal stability and electrical resistivity of Ag films.

*E-mail address: kawamumd@mail.kitami-it.ac.jp

1. Introduction

Silver (Ag) with the lowest electrical resistivity (ρ = 1.59 μΩ cm at 293 K) [1] is the potential candidate for electrodes and metallization materials in various electronic devices. [2-5] However, Ag thin films on insulating oxide substrates are prone to agglomerate at high temperatures, which makes the films discontinuous, followed by an abrupt increase in electrical resistivity. [6-8] In order to take full advantage of Ag thin films, the improvement in the thermal stability of Ag thin films seems very important. Although the mechanism of Ag agglomeration is complex, ease of Ag atom migration and poor adhesion of the Ag thin film on the silicon dioxide (SiO_2) or glass substrate have been generally considered to be the cause. [9-12] Over the past decade, many reports have focused on the issue of agglomeration suppression, and one proposed solution was to alloy Ag with other metals. [13-16] Unfortunately, even alloying a relative low content of other metals could lead to an obvious increase in electrical resistivity owing to the impurity scattering effect. Recently, it has been reported that the Ag films with only interface layers of other materials could achieve a lower electrical resistivity than alloy films and a good thermal stability. [5,9,17,18] However, we previously confirmed that the sandwich structure of Ag films with both the surface and interface layers was more effective than the double-layer structure. [11,19]

Based on a previous work on Ag thin films with titanium (Ti) surface and interface layers, namely, the Ti/Ag/Ti structure, [19] related research studies have been further carried out. In the present study, we selected niobium (Nb) and Ti as the surface and interface layers, respectively. Nb with lower bulk resistivity (ρ = 12.5 μΩ cm at 293 K) [1] and larger Gibbs free energy to form Nb_2O_5 ($\Delta_f G°$ = -1766 kJ/mol) [20] than Ti (ρ = 42.0 μΩ cm at 293 K [1] and $\Delta_f G°$ = -939.7 kJ/mol for the formation of TiO_2 [20]) was

expected to exhibit a better effect as a capping layer. On the other hand, although the role of the Ti interface layer in the Ti/Ag/Ti films was simply discussed previously,[19] in order to investigate the effects of the Ti interface layer in detail, the Ag films with only the Ti interface layer, namely, Ag/Ti, were considered as research objects. Finally, the properties of the Ag film with both the Nb surface and Ti interface layers, namely, Nb/Ag/Ti, were evaluated.

2. Experimental Procedure

The multilayered films were prepared by rf magnetron sputtering. After the system was evacuated to below 1.8×10^{-5} Pa, argon gas was introduced at a flow rate of 0.76 ml/min. The gas pressure was fixed at 1.03 Pa, the distance between the substrate and the target was fixed at 55 mm, and the Ag (99.99% purity), Nb (99.9% purity) and Ti targets (99.99% purity) were used in a certain order during the deposition process. A Si (001) wafer with a 100-nm-thick thermally grown SiO_2 layer was used as the substrate without heating during sputtering. In this study, the films of pure Ag (100 nm), Nb (60 nm), Ti (60 nm), Nb (1 – 10 nm)/Ag (100 nm), Ag (100 nm)/Ti (1 – 10 nm) and Nb (5 nm)/Ag (100 nm)/Ti (3 nm) were investigated, and another Nb (5 nm)/Ag (100 nm)/Nb (5 nm) film prepared this time and Ti (3 nm)/Ag (100 nm)/Ti (3 nm) film prepared previously were used for comparison. All the deposited films were preserved in an air desiccator before annealing. Annealing was conducted at 500 or 600 °C in a lamp-heating furnace for 1 h after evacuation to below 1.0×10^{-4} Pa.

In addition, in order to clarify the role of the Nb surface layer, another series of experiments were carried out. The films of Ag (50 nm) and Nb (3 nm)/Ag (50 nm) were deposited at room temperature. After deposition, the substrate was not taken out but

annealed at 450 °C (the extreme temperature of the heater) in the sputtering chamber with the evacuation of below 1.8×10^{-5} Pa. For comparison, another Nb(3 nm)/Ag(50 nm) film was deposited and kept in air before annealing in the furnace at 450 °C.

The film thickness was estimated using multibeam interferometry. The surface morphology of the films was observed by scanning electron microscopy (SEM) and atomic force microscopy (AFM). The crystal structure was determined by X-ray diffraction (XRD) analysis using Cu Kα radiation. X-ray photoelectron spectroscopy (XPS) analysis was carried out to investigate the chemical bonding state of the elements at the surface. Microscratch tests (scratch speed: 10 μm/s; loading rate: 2.67 mN/s) were carried out to evaluate the adhesion of the thin film on the SiO_2/Si substrate. The electrical resistivity was measured at room temperature by the four-point probe method.

3. Results and Discussion

3.1 Ag film with Nb surface layer (Nb/Ag film)

Figure 1 shows the SEM micrographs of the pure Ag, Nb, and Nb (1 – 10 nm)/Ag films after annealing at 600 °C in the lamp-heating furnace. The pure Ag film suffered from severe agglomeration during annealing, which resulted in the exposure of a large substrate area. However, the pure Nb film with a thickness of only 60 nm exhibited an excellent thermal stability. This is because the crystal cohesive energy of Nb (730 kJ/mol) is much larger than that of Ag (284 kJ/mol),[21] and Ag atoms can migrate more easily by absorbing energy at high temperatures, which causes agglomeration. The Nb (1 nm)/Ag film was agglomerated, although its dewetted area was smaller than that of the pure Ag film. It was observed that a 1-nm-thick Nb layer was not enough to suppress the agglomeration of the Ag film. The morphological stability was

significantly improved by increasing the thickness of the Nb surface layer to 3 nm or above, and the Nb surface layers with thicknesses of 5 nm and above appeared to be more effective for agglomeration suppression judging from the small amount and area of voids formed after annealing. The roughnesses of the pure Ag and Nb (5 nm)/Ag films were further investigated by AFM after annealing at 600 °C, and their rms roughnesses were 26.7 and 2.3 nm, respectively. It was shown that the surface of the Nb/Ag films, except where there were voids, appeared very flat.

It is important to keep the electrical resistivity of the Ag thin films low as well as to enhance their thermal stability. Figure 2 shows the change in the electrical resistivity of the Ag films with different Nb surface layer thicknesses as a function of annealing temperature. Unlike the Ag-Nb alloy films studied previously,[8] there was no effect of impurity scattering on the resistivity of the Nb/Ag films even after annealing, because Nb was very difficult to dissolve in Ag or react with Ag.[22] The resistivity of the as-deposited Nb/Ag films increased slightly with increasing Nb surface layer thickness only because of the bulk resistivity of Nb being higher than that of Ag. However, the change in resistivity with increasing Nb surface layer thickness was found to be smaller than that of Ti/Ag films by comparing with the previous results.[19] That was because the bulk resistivity of Nb was much lower than that of Ti as mentioned above. The resistivities of all the films decreased after annealing at 500 °C owing to the improvement in film crystallinity and the relatively smooth film surface. The resistivities of the pure Ag and Nb (1 nm)/Ag films increased markedly after annealing at 600 °C, because the severe agglomeration made the films discontinuous as a result of their poor thermal stability. However, the Nb (3 – 10 nm)/Ag films could maintain a low resistivity even after annealing at 600 °C, and there was scarcely any difference in

resistivity between the Nb (3 nm)/Ag and Nb (5 nm)/Ag films. Therefore, from the standpoint of good morphological stability and low electrical resistivity, 5 nm was thought to be the optimum thickness for the Nb surface layer.

Next, we discussed the mechanism of agglomeration suppression of the Nb/Ag film. Similarly to the roles of aluminum or titanium surface layers on Ag films, [11,19] the formation of the Nb oxide surface layer as a passivation layer was considered to be the main factor for agglomeration suppression. The chemical bonding states of the surface layer on the Nb (3 nm)/Ag films obtained before and after annealing were analyzed by XPS, as shown in curves (a) and (b) of Fig. 3. The binding energy of the main peaks in both as-deposited and annealed samples is 207.4 eV, which is equal to that of the Nb_2O_5 reference (207.5 eV). [23] A few low-valence Nb oxides were also detected in all the samples. In addition, a weak peak belonging to the Nb metal [23] only existed in the as-deposited film. The above results showed that most of Nb was oxidized by the natural oxidation before annealing, and the residual Nb was completely oxidized by the oxygen molecules adsorbed on the surface and the residual oxygen in the furnace during annealing. The Nb oxide surface layer was considered to play an important role in preventing the migration of Ag atoms during annealing. We doubted whether oxidation was necessary for Nb to suppress the agglomeration of the Ag films. Because the 60-nm-thick Nb film was difficult to agglomerate and keep continuous and flat after annealing at 600 °C, the Nb metal surface nano layer would have the same effect on agglomeration suppression. In order to prevent the oxidation of the thin Nb layer in air before annealing, the additional experiments, where the pure Ag (50 nm) and Nb (3 nm)/Ag (50 nm) films were annealed consecutively in the sputtering chamber after deposition, were carried out. As we know, the temperature of agglomeration occurrence

decreases abruptly with decreasing Ag film thickness. [24] Because the annealing temperature was set to 450 °C owing to the limitation of the heater in the sputtering chamber, Ag film thickness was fixed to 50 nm to induce agglomeration. Curve (c) in Fig. 3 showed that there was a large amount of Nb metal in the surface layer of the Nb/Ag film after annealing in the sputtering chamber. The existence of Nb oxide was considered to be the result of natural oxidation by exposure to air before XPS analysis. Figure 4 shows the SEM images of the Ag and Nb (3 nm)/Ag films directly annealed in the sputtering chamber, and another Nb (3 nm)/Ag film taken out of the chamber and annealed in the lamp-heating furnace. The Ag (50 nm) film was completely agglomerated after annealing at 450 °C. In contrast, the other films with the Nb metal and Nb oxide surface layers, respectively, exhibited almost the same thermal stability. Therefore, no matter what the state of Nb was, the Nb surface layer was found to be effective for agglomeration suppression.

3.2 Ag film with Ti interface layer (Ag/Ti film)

The SEM micrographs of the Ag/Ti (1 – 10 nm) films annealed at 600 °C in the lamp-heating furnace are shown in Fig. 5. Although the surface morphology of the annealed Ag/Ti (1 nm) film was much better than that of the Ag film, as shown in Fig. 1 (a), the 1-nm-thick Ti layer seemed to be less effective for restraining the growth of voids than the Ti layers with thicknesses of 3 nm and above. In addition, the AFM analysis showed that the rms roughness of parts of the surface without voids for Ag/Ti (1 nm) was 8.2 nm, which was larger than that of the Ag/ Ti (3– 10 nm) films ranging from 3.5 to 4.3 nm. It was suggested that the morphological stability of the Ag films deposited on the Ti (3 – 10 nm) interface layers was greatly improved. However, the

effect of the Ti interface layer on the thermal stability of the Ag film was found to be inferior to that of the Nb surface layer by comparing it with the results indicated in the previous section.

Figure 6 shows the electrical resistivities of the pure Ag and Ag/Ti films as a function of annealing temperature. The resistivities of all the Ag/Ti films certainly decreased after annealing at 500 °C, but slightly increased with increasing annealing temperature to 600 °C caused by agglomeration occurring to some extent. Another interesting result was that the resistivities of the as-deposited Ag/Ti (3 – 10 nm) films were almost the same, and approximately 0.2 μΩ cm lower than that of the pure Ag film. The possible reason for this would be explained in the following.

Ti was usually used as an underlying material for enhancing the adhesion of other films to the SiO_2 substrates [9,25] resulting from a large affinity for Ti and oxygen, which was expected to positively affect the agglomeration suppression of Ag films. In this study, the adhesion strengths of the Ag and Ag/Ti films on the SiO_2 substrates were investigated, as shown in Fig. 7. It was proved that, by inserting a Ti interface layer, the adhesion strength was increased to about four times that of the Ag film on the SiO_2 substrate. After XRD analysis, the Ti interface layer appeared to have another role, which was beneficial for agglomeration suppression. The results showed that the XRD patterns of both the Ag and Ag/Ti (1 nm) as-deposited films consisted of Ag(111) and Ag(200) peaks in spite of the much higher peak intensity of Ag(111) than that of Ag(200); however, the Ag(200) peak disappeared completely with increasing Ti interface layer thickness to 3nm and above. The full width at half maximum (FWHM) of the XRD rocking curve was further investigated to evaluate the crystalline orientation of Ag(111) in the as-deposited Ag and Ag/Ti films, as shown in Fig. 8. The Ag/Ti (3 –

10 nm) films showed an equally higher crystalline orientation of Ag(111), which is the close-packed plane for the face-centered cubic structure of Ag. The XRD pattern of the pure Ti film deposited on the SiO_2 substrate showed that the hexagonal close-packed Ti film mainly grew towards <0002> preferentially. It is well known that any three neighboring atoms closely link and form an equilateral triangle at the close-packed plane of the hexagonal and face-centered cubic structures. The distances between two neighboring atoms at the close-packed Ti(0002) and Ag(111) planes were 0.2944 [26] and 0.2888 nm [27], respectively, and the mismatch of axial length was only 1.9%. Therefore, it was easy for the Ag(111) plane to locate on the Ti(0002) plane. However, the Ag films deposited on the amorphous SiO_2 substrates showed a poor preferred orientation of (111). The maximum profile height difference of the 1-nm-thick Ti layer deposited on the SiO_2 substrate was proved to be close to 1 nm by AFM analysis, as shown in Fig. 9, which suggested that the 1-nm-thick Ti layer was not continuous on the flat SiO_2 substrate. Therefore, Ag/Ti (1 nm) exhibited no marked improvement in the crystalline orientation of Ag(111). In contrast, the substrate could be completely covered by the Ti layer with a thickness of 3 nm or above because of the profile depth being smaller than the thickness of the Ti layer, as shown in Fig. 9, which contributed to the improvement in the crystalline orientation of Ag(111). Ag(111) is the close-packed plane with minimum surface energy, and the enhancement of Ag(111) was once found to be an important factor for the improvement in the thermal stability of Ag films by Kim *et al.* [14] . On the other hand, it was observed that there were no significant change in the surface roughness and grain size of Ag(111), and no impurities inside the pure Ag and Ag/Ti films; thus, only the change in the crystalline orientation of Ag(111) could lead to the same tendency of the electrical resistivity change of the as-deposited films.

Therefore, we considered that the highly oriented Ag films had a lower electrical resistivity. Consequently, the Ti(3 – 10 nm) layer could improve the thermal stability and reduce the resistivity of the overcoated Ag.

3.3 Nb/Ag/Ti multilayered films

On the basis of the discussion above, the 5-nm-thick Nb surface layer and 3-nm-thick of Ti interface layer were sufficient for the improvement in the overall performance of the Ag films. Therefore, the Nb (5 nm)/Ag/Ti (3 nm) multilayered film was expected to be the best combination. The morphological stability and electrical resistivity of the Nb (5 nm)/Ag (100 nm)/Ti (3 nm), Nb (5 nm)/Ag (100 nm)/Nb (5 nm), and Ti (3 nm)/Ag (100 nm)/Ti (3 nm) films were evaluated, as shown in Figs. 10 and 11, respectively. It was suggested that the Nb (5 nm)/Ag/Ti (3 nm) film was better than the double-layer films in terms of thermal stability and resistivity. On the other hand, it was found that the Nb (5 nm)/Ag/Ti (3 nm) film had a higher morphological stability than the Nb (5 nm)/Ag/Nb (5 nm) film and a lower resistivity than the Nb (5 nm)/Ag/Nb (5 nm) and Ti (3 nm)/Ag/Ti (3 nm) films. It was indicated that Nb and Ti were suitable for the surface and interface layers, respectively. Therefore, Ag films with different materials of more appropriate surface and interface layers could obtain a higher thermal stability and a lower electrical resistivity than Ag films with the same materials of surface and interface layers.

4. Conclusions

The Nb surface layer, regardless of the chemical state of metal or oxide, restrained the migration of Ag atoms during annealing, which contributed to agglomeration

suppression. From the standpoint of thermal stability and electrical resistivity, the 5-nm-thick Nb layer was an appropriate capping layer. Ti interface layers not only improved the adhesion between Ag films and SiO_2 substrates but also induced the growth of the (111) single oriented Ag film. Therefore, Ag films with Ti interface layer thickness of 3 nm or above exhibited a low resistivity and a relatively good thermal stability. Finally, it was confirmed that the triple-layer film of Nb (5 nm)/Ag/Ti (3 nm) was superior to the double-layer films in achieving both good thermal stability and low electrical resistivity. Different materials of more appropriate surface and interface layers could promote a higher thermal stability and a lower electrical resistivity in Ag films than the same materials of surface and interface layers.

Acknowledgement

This research was supported by a Grant-in-Aid for Scientific Research C (No. 22560712) from the Japan Society for the Promotion of Science.

References

1) The Chemical Society of Japan: *Kagaku Binran* (Handbook of Chemistry) (Maruzen, Tokyo, 1993) 4th ed., Vol. 2, p. 490 [in Japanese].

2) T. Fudei, M. Kawamura, Y. Abe, and K. Sasaki: J. Nanosci. Nanotechnol. **12** (2012) 1188.

3) M. Kawamura, D. Fukuda, Y. Inami, Y. Abe, and K. Sasaki: J. Vac. Sci. Technol. A **27** (2009) 975.

4) T. L. Alford, P. Nguyen, Y. Zeng, and J. W. Mayer: Microelectron. Eng. **55** (2001) 383.

5) Y. S. Jung, Y. W. Choi, H. C. Lee, and D. W. Lee: Thin Solid Films **440** (2003) 278.

6) K. Sugawara, M. Kawamura, Y. Abe, and K. Sasaki: Microelectron. Eng. **84** (2007) 2476.

7) K. Sugawara, Y. Minamide, M. Kawamura, Y. Abe, and K. Sasaki: Vacuum **83** (2009) 610

8) Y. Minamide, M. Kawamura, Y. Abe, and K. Sasaki: Vacuum **84** (2010) 657.

9) Z. Wang, X. Cai, Q. Chen, and P. K. Chu: Thin Solid Films **515** (2007) 3146.

10) M. Kawamura, T. Fudei, Y. Abe, and K. Sasaki: Jpn. J. Appl. Phys. **48** (2009) 118002.

11) M. Kawamura, Y. Inami, Y. Abe, and K. Sasaki: Jpn. J. Appl. Phys. **47** (2008) 8917

12) T. L. Alford, L. Chen, and K. S. Cadre: Thin Solid Films **429** (2003) 248.

13) T. L. Alford, D. Adams, T. Laursen, and B. M. Ullrich: Appl. Phys. Lett. **68** (1996) 3251.

14) H. C. Kim and T. L. Alford: J. Appl. Phys. **94** (2003) 5393.

15) E. E. Glickman, V. Bogush, A. Inberg, Y. Shacham-Diamand, and N. Croitoru:

Microelectron. Eng. **70** (2003) 495.

16) M. Kawamura, M. Yamaguchi, Y. Abe, and K. Sasaki: Microelectron. Eng. **82** (2005) 277.

17) G. F. Malgas, D. Adams, T. L. Alford, and J. W. Mayer: Thin Solid Films **467** (2004) 267.

18) T. Guan and R. Puers: Procedia Eng. **5** (2010) 1356.

19) M. Kawamura, Z. Zhang, R. Kiyono, and Y. Abe: to be published in Vacuum.

20) The Chemical Society of Japan: *Kagaku Binran* (Handbook of Chemistry) (Maruzen, Tokyo, 1993) 4th ed., Vol. 2, pp. 291-293 [in Japanese].

21) C. Kittel: *Introduction to Solid State Physics* (Wiley, New Caledonia, 2005) 8th ed., p. 50.

22) M. R. Baren: Bull. Alloy Phase Diagrams **10** (1989) 640.

23) J. F. Moulder, W. F. Stickle, P. E. Sobol, and K. D. Bomben: *Handbook of X-ray Photoelectron Spectroscopy* (Perkin-Elmer, Eden Prairie, MN, 1992) p. 229.

24) H. C. Kim, T. L. Alford, and D. R. Allee: Appl. Phys. Lett. **81** (2002) 4287.

25) M. Mashita and M. Yoshida: *Hakumaku Kougaku Handbook* (Handbook of Film Technology) (Kodansha, Tokyo, 1998) p. 380 [in Japanese].

26) ICDD, PDF-2, 00-089-5009 (2009).

27) ICDD, PDF-2, 00-089-3722 (2009).

Figures:

Fig. 1 SEM images of the films after annealing at 600 °C in the lamp-heating furnace. (a) pure Ag (100 nm), (b) pure Nb (60 nm), (c) Nb (1 nm)/Ag (100 nm), (d) Nb (3 nm)/Ag (100 nm), (e) Nb (5 nm)/Ag (100 nm), and (f) Nb (10 nm)/Ag (100 nm) films.

Fig. 2 (Color online) Resistivities of pure Ag (100 nm) and Nb (1 – 10nm)/Ag (100 nm) films as a function of annealing temperature.

Fig. 3 (Color online) Nb 3d XPS spectra for the surfaces of the films. (a) As-deposited Nb (3 nm)/Ag (100 nm) film, (b) Nb (3 nm)/Ag (100 nm) film annealed at 500 °C in the lamp-heating furnace, and (c) Nb (3 nm)/Ag (50 nm) film annealed at 450 °C in the sputtering chamber.

Fig. 4 SEM images of the films after annealing at 450 °C. (a) Pure Ag (50nm) film annealed in the sputtering chamber, (b) Nb (3 nm)/Ag (50 nm) film annealed in the sputtering chamber, and (c) Nb (3 nm)/Ag (50 nm) film annealed in the lamp-heating furnace.

Fig. 5 SEM images of the films after annealing at 600 °C in the lamp-heating furnace. (a) Ag (100 nm)/Ti (1 nm), (b) Ag (100 nm)/Ti (3 nm), (c) Ag (100 nm)/Ti (5 nm), and (d) Ag (100 nm)/Ti (10 nm) films.

Fig. 6 (Color online) Resistivities of pure Ag (100 nm) and Ag (100 nm)/Ti (1 – 10nm) films as a function of annealing temperature.

Fig. 7 Critical delamination load of the as-deposited Ag (100 nm)/Ti (1 – 10nm) films as a function of the Ti interlayer thickness.

Fig. 8 (Color online) XRD rocking curves of the as-deposited Ag (100 nm) and Ag (100 nm)/Ti (1 – 10nm) films.

Fig. 9 AFM line profiles of SiO_2 substrate and Ti (1 nm)/SiO_2 and Ti (3 nm)/SiO_2

monolayer films.

Fig. 10 SEM images of the films after annealing at 600 °C in the lamp-heating furnace. (a) Nb (5 nm)/Ag (100 nm)/Ti (3 nm), (b) Nb (5 nm)/Ag (100 nm)/Nb (5 nm), and (c) Ti (3 nm)/Ag (100 nm)/Ti (3 nm) films.

Fig. 11 (Color online) Resistivities of pure Ag (100 nm), Nb (5 nm)/Ag (100 nm), Ag (100 nm)/Ti (3 nm), Ti (3 nm)/Ag (100 nm)/Ti (3 nm), Nb (5 nm)/Ag (100 nm)/Nb (5 nm), and Nb (5 nm)/Ag (100 nm)/Ti (3 nm) films as a function of annealing temperature.

Fig. 1

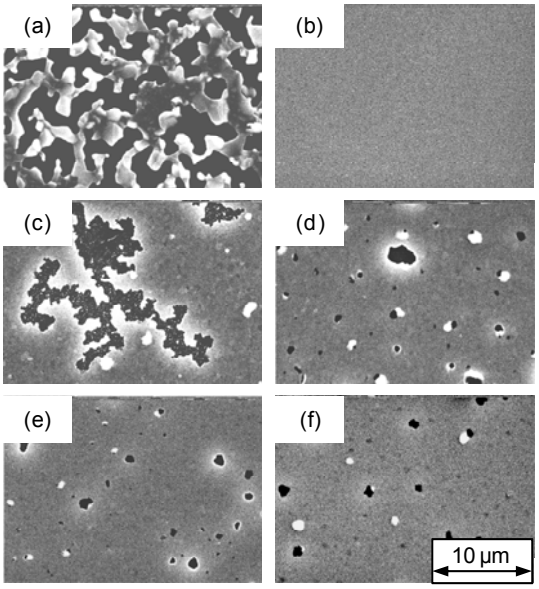

Fig. 2

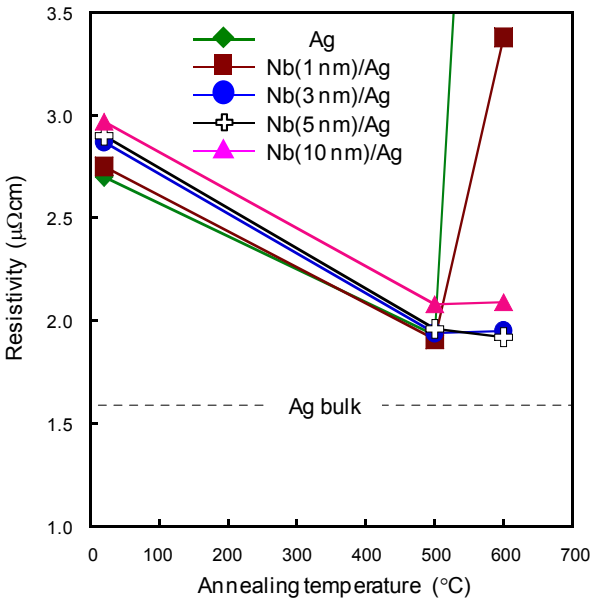
Ag
Nb(1 nm)/Ag
Nb(3 nm)/Ag
Nb(5 nm)/Ag
Nb(10 nm)/Ag
Ag bulk
Resistivity (μΩcm)
Annealing temperature (°C)
3.5
3.0
2.5
2.0
1.5
1.0
0
100
200
300
400
500
600
700

Fig. 3

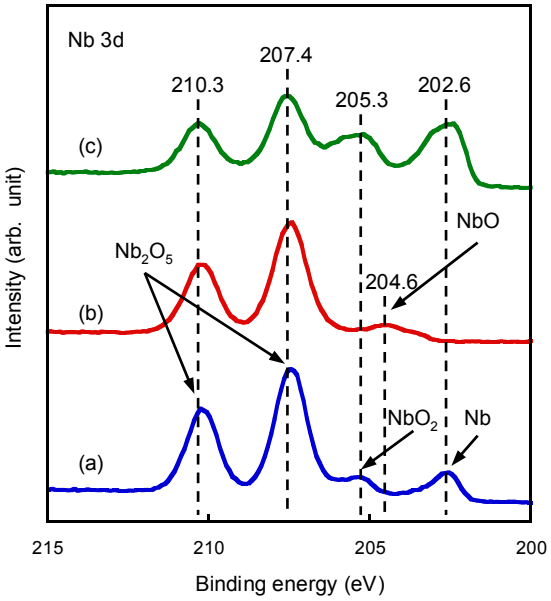
Nb 3d
207.4
210.3
205.3
202.6
(c)
NbO
Nb_2O_5
204.6
(b)
NbO_2
Nb
(a)
Intensity (arb. unit)
215
210
205
200
Binding energy (eV)

Fig. 4

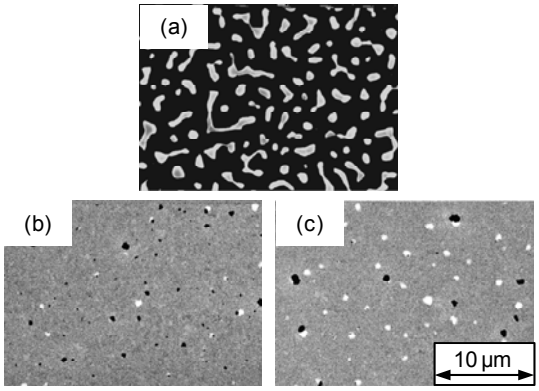

Fig. 5

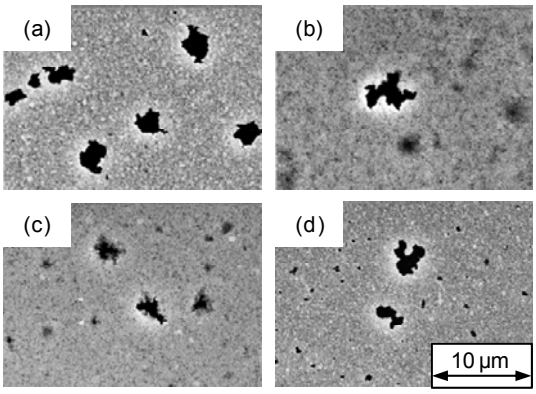

Fig. 6

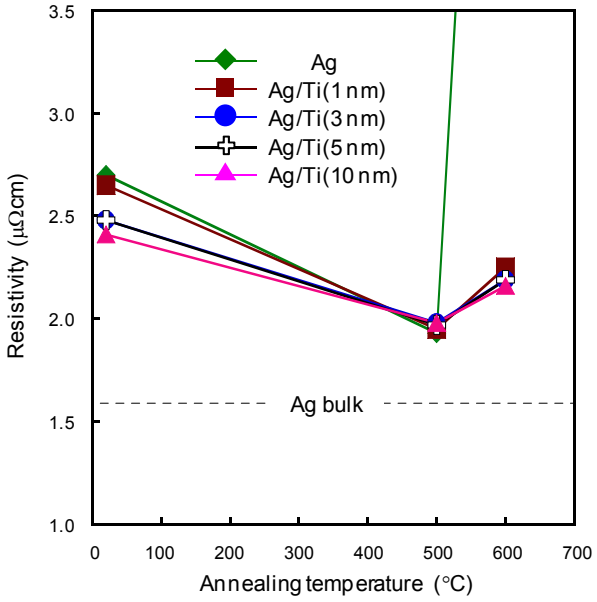
Ag
Ag/Ti(1 nm)
Ag/Ti(3 nm)
Ag/Ti(5 nm)
Ag/Ti(10 nm)
Ag bulk
Resistivity (μΩcm)
Annealing temperature (°C)
3.5
3.0
2.5
2.0
1.5
1.0
0
100
200
300
400
500
600
700

Fig. 7

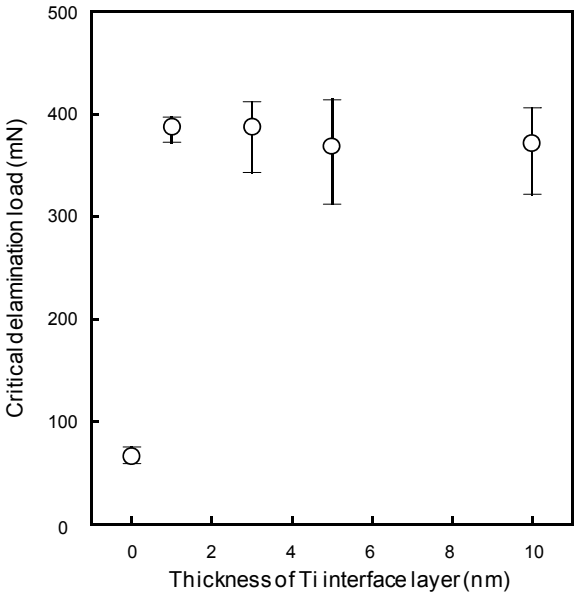
500
400
300
200
100
0
Critical delamination load (mN)
0
2
4
6
8
10
Thickness of Ti interface layer (nm)

Fig. 8

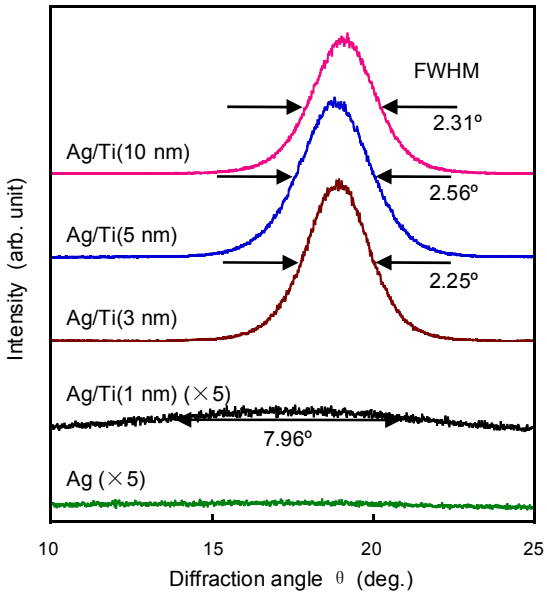
FWHM
2.31°
Ag/Ti(10 nm)
2.56°
Ag/Ti(5 nm)
2.25°
Ag/Ti(3 nm)
Ag/Ti(1 nm) (×5)
7.96°
Ag (×5)
Intensity (arb. unit)
10
15
20
25
Diffraction angle θ (deg.)

Fig. 9

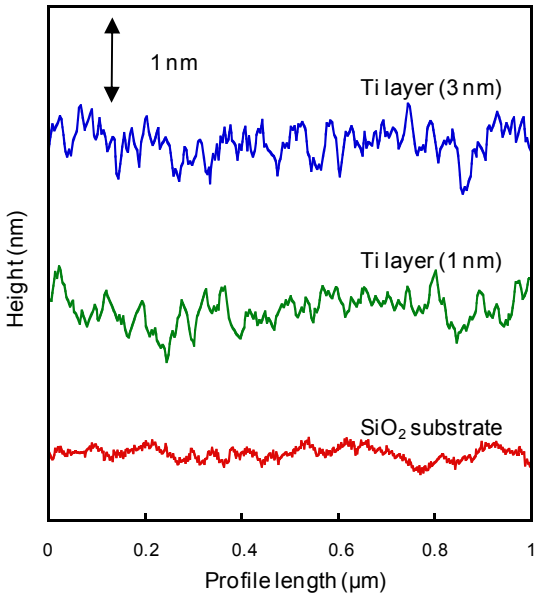
1 nm
Ti layer (3 nm)
Ti layer (1 nm)
SiO2 substrate
Height (nm)
0
0.2
0.4
0.6
0.8
1
Profile length (μm)

Fig. 10

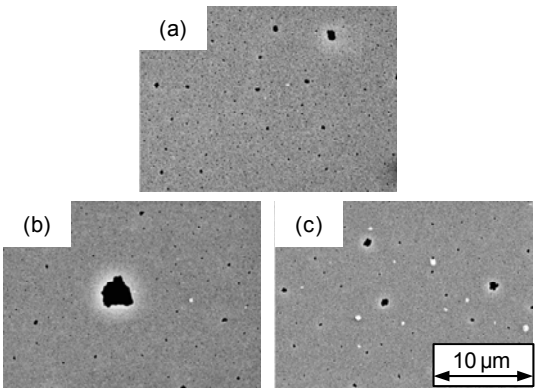

Fig. 11

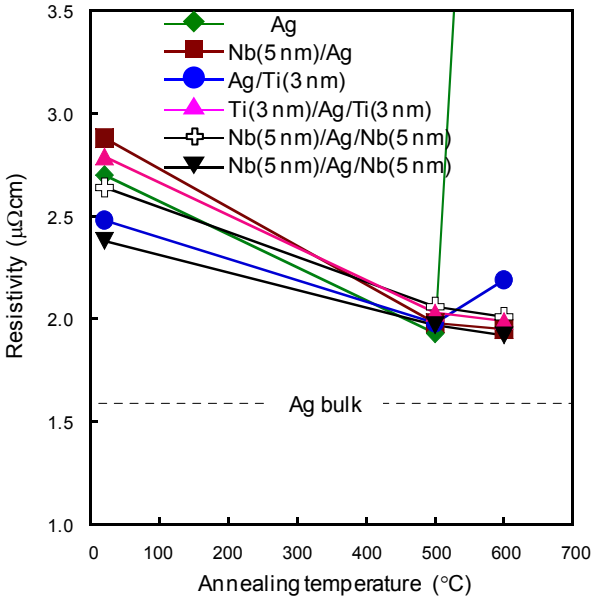
Ag
Nb(5 nm)/Ag
Ag/Ti(3 nm)
Ti(3 nm)/Ag/Ti(3 nm)
Nb(5 nm)/Ag/Nb(5 nm)
Nb(5 nm)/Ag/Nb(5 nm)
Ag bulk
Resistivity (μΩcm)
Annealing temperature (°C)
3.5
3.0
2.5
2.0
1.5
1.0
0
100
200
300
400
500
600
700